Driving and Controlling Molecular Surface Rotors with a Terahertz Electric Field

Jan Neumann,[†] Kay E. Gottschalk,[†,§] and R. Dean Astumian[‡,*]

[†]Chair for Applied Physics, Ludwig-Maximilians-University Munich, Amalienstraße 54, Munich, 80799, Germany and [‡]University of Maine, Orono, Maine, United States. [§]Present address: Experimental Physics, Ulm University, D-89069 Ulm, Germany.

ABSTRACT

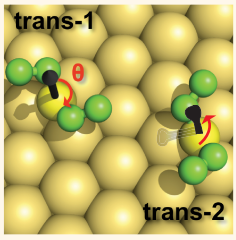

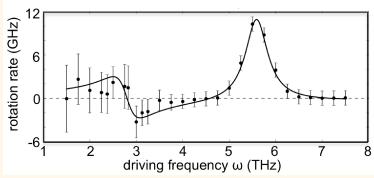

Great progress has been made in the design and synthesis of molecular motors and rotors. Loosely inspired by biomolecular machines such as kinesin and the FoF1 ATPsynthase, these molecules are hoped to provide elements for construction of more elaborate structures that can carry out tasks at the nanoscale corresponding to the tasks accomplished by elementary machines in the macroscopic world. Most of the molecular motors synthesized to date suffer from the drawback that they operate relatively slowly (less than kHz). Here we show by molecular dynamics studies of a diethyl sulfide rotor on a gold(111) surface that a high-frequency oscillating electric field normal to the surface can drive directed rotation at GHz frequencies. The maximum directed rotation rate is 10^{10} rotations per second, significantly faster than the rotation of previously reported directional molecular rotors. Understanding the fundamental basis of directed motion of surface rotors is essential for the further development of efficient externally driven artificial rotors. Our results represent a step toward the design of a surface-bound molecular rotary motor with a tunable rotation frequency and direction.

KEYWORDS: surface rotor · Brownian machine · oscillating field · directed rotation · frequency control · directional switching

Control of directional motion at the molecular level is one of the great overarching themes of nanoscience.[1−4] Captivated by the mechanisms of biological molecular pumps, motors, and rotors, synthetic chemists have recently made great progress in the design and synthesis of molecular machines, including motors,[5] rotors,[6,7] and steppers[8] that exploit, rather than fight against, ineluctably present thermal noise.[9,10] Most of these molecular machines, however, operate only relatively slowly, at or below the MHz regime.[11] Recently, Garcia-Garibay and colleagues[12] reported on the synthesis and characterization of a halogen-bonded crystal with a degree of freedom having a rotation frequency of several GHz, but the rotation is directionless, with equal probability in the clockwise and counterclockwise directions. A key goal in construction of a functional molecular machine is to design a mechanism for inputting energy to drive rapid directed rotation. Chemical driving[13] suffers from diffusional limitations and seems limited to the 10−100 kHz range, consistent with biomolecular machines driven by, for example, hydrolysis of ATP. Light[14] offers another possibility,[15] but optically driven devices may be limited by the finite number of excitation/de-excitation cycles a molecule can undergo before breaking down. Here we discuss driving directed rotation with externally applied high-frequency electric fields.[16] In contrast to mechanisms involving absorption of light (which is indeed an oscillating electromagnetic field), the driving mechanism described here is classical and involves realignment of dipoles as the electric field changes rather than absorption in which electrons undergo transitions between discrete energy levels or where quantized vibrational modes are excited. The frequencies studied here (1−10 THz) fall in the microwave to far-infrared region of the electromagnetic spectrum.

Inspired by low-temperature single-molecule STM experiments on the rotational dynamics of thioether surface rotors[17,18] we carried out room-temperature (300 K) molecular dynamics studies[19,20] of a diethyl sulfide (DES) rotor on a gold(111) surface under the influence of a high-frequency (THz) oscillating electric field normal to the gold surface. The ac field can drive directed rotation that depends on the conformational state of the molecule and on the frequency and amplitude of the field. We interpret the mechanism of the field-induced directed rotation in terms of the dependence of the energy landscape of the

* Address correspondence to astumian@maine.edu.

Received for review March 7, 2012 and accepted May 10, 2012.

Published online May 10, 2012
10.1021/nn301001s

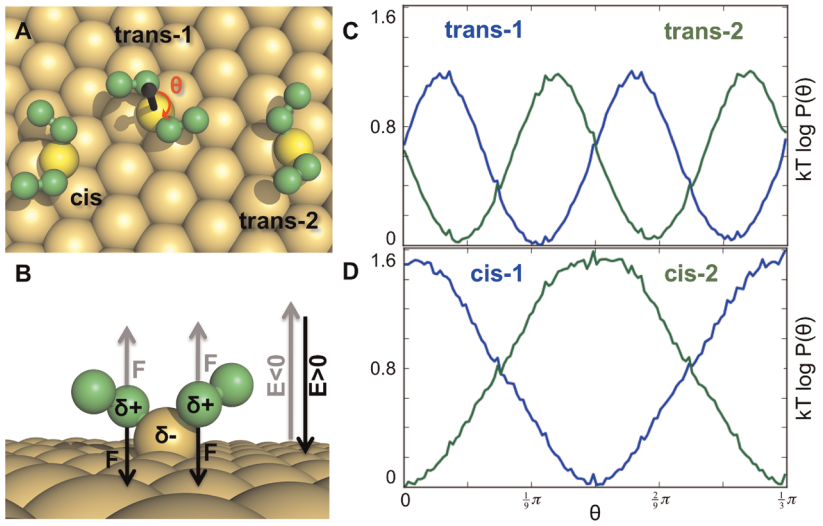

Figure 1. (A) Conformations (cis, trans-1, and trans-2) of the diethyl sulfide rotor bound in an fcc position to the gold (111) surface . The angle θ (red) around the rotation axis (black) is explicitly illustrated for the trans-1 conformation. (B) An electric field acts on the partial charges of the rotor to force the rotor arms slightly away from or toward the surface. (C) Plot of the logarithm of the probability density, and hence of the free energy landscape, of the freely rotating trans-1 (blue) and trans-2 (green) conformations. (D) Plot of the logarithm of the probability density of freely rotating cis-1 (blue) and cis- (green) conformations.

different rotor conformations on the static electric field strength. Cycling through in themselves symmetric energy landscapes creates a time-dependent asymmetry in the population of the rotor angles. The frequency dependence can be well fit by a response function that is the sum of an out-of-phase component at the characteristic frequency of the rotor and an in-phase component at twice the characteristic frequency of the rotor. The THz field induces GHz rotation of the molecular rotor, making the DES/gold system the fastest directed rotor (by far) described to date.

RESULTS

The motion of a DES rotor on a gold(111) surface was investigated using molecular dynamics (MD) simulations with DFT-optimized GolP parameters.[21] In contrast to dimethyl sulfide, where the sulfur binds most stably in an atop position,[22] the sulfur in the diethyl sulfide studied here was most stably bound in an fcc position to the gold. We held the sulfur in this symmetric position in our MD simulations, forming a stationary rotation axis (Figure 1A). By analyzing the free rotation of the rotor we identified four major conformations, two trans- and two cis-isomers (Figure 1A), that can be classified by two dihedral angles, $\delta_1(C^1{-}C^2{-}S{-}C^3)$ and $\delta_2(C^2{-}S{-}C^3{-}C^4)$, along the backbone of the DES molecule ($C^1H_3{-}C^2H_2{-}S{-}C^3H_2{-}C^4H_3$). The two cis-forms, cis-1 ($\delta_1 < 0$, $\delta_2 > 0$) and cis-2 ($\delta_1 > 0$, $\delta_2 < 0$), are interconverted by rotation about an axis normal to the gold surface. The two trans-isomers, trans-1 ($\delta_1 < 0$, $\delta_2 < 0$) and trans-2 ($\delta_1 > 0$, $\delta_2 > 0$), cannot be converted into one another by rotation about an axis normal to the gold surface. Simulations of free rotation for several different static field strengths ranging from -9 to $+9$ V/nm were carried out. The mean lifetimes in the cis- and trans-states varied significantly with the field, as shown in Table 1. These data were calculated by analysis of a number of trajectories with a total time of 0.2 ms. With an attempt frequency of 10^{12} s^{-1} the lifetime at zero field is consistent with an activation energy of 5−10 kJ/mol, a value that is in line with a C−C torsion bond potential.

TABLE 1. Lifetimes *vs* Field

field (V/nm)	τ_{cis} (ps)	τ_{trans} (ps)
−9	1.2	7.52
−6	1.97	11.45
−3	3.48	20.38
0	7.7	51
+3	15.81	94.27
+6	51.79	262.60
+9	295.45	850.06

In our initial studies of the rotational motion under the influence of an oscillating field we noticed that sometimes the rotor turned clockwise, sometimes counterclockwise, and sometimes the rotation was not directed at all. Generally the direction of rotation remained the same during an entire trajectory, although we sometimes observed that the direction of rotation would abruptly change. At first we ascribed this behavior to a residual inertial effect and the switching of the direction to the effects of noise, but this explanation was ruled out by showing that the net rotation in all cases stopped very quickly when the field was turned off. Eventually we were able to correlate the behavior at a given frequency with the conformational state of the molecule. Because of the length of simulation possible with the oscillating field (5 ns), the conformation was generally, but not always, constant during simulation of a single trajectory. Due to computational constraints, it

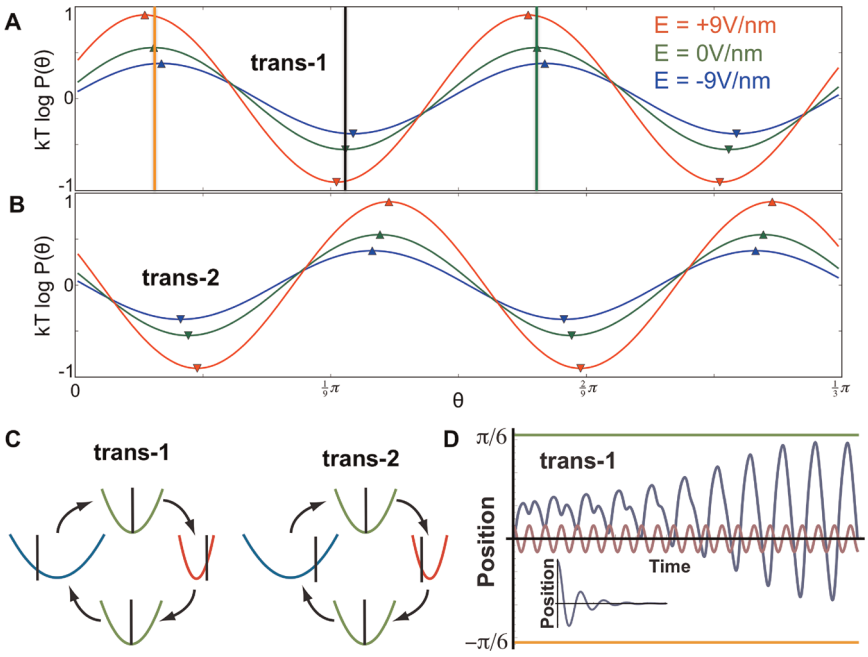

Figure 2. Free energy landscapes at $E = +9$ V/nm (red), at $E = 0$ V/nm (green), and at $E = -9$ V/nm (blue) for trans-1 (A) and trans-2 (B) are shown. The electric field shifts the phase (i.e., the positions of minima and maxima indicated by triangles) and modulates the amplitude. The orange, black, and green lines correspond to the $-\pi/6$, 0, and $\pi/6$ positions and are reflected in panel D. (C) Schematic illustration of the motion of an energy minimum in the harmonic approximation. For trans-1, the minimum shifts to the left when the spring constant is large and to the right when the spring constant is small. For trans-2, the minimum shifts to the right when the spring constant is large and to the left when the spring constant is small. (D) Deterministic simulation of eq 1. External driving field (violet) and angle position of the rotor (blue) are shown. The inset shows the damped relaxation of the rotor position when the field is turned off.

was not practical to simulate a long enough trajectory that the molecule undergoes many conformational transitions during a single run. Thus we decided to investigate the behavior of the different conformational states of the molecule separately where during a single trajectory the dihedral angle of the rotor was restrained to within $\pm\pi/9$ radians to prevent transition to a different conformational state. This allowed us to focus on the almost 1-D motion of the rotor around an axis perpendicular to the gold surface piercing the center of the sulfur atom. The equation of motion for a 1-D surface rotor with noise is $I\ddot{\theta} + \Gamma\dot{\theta} - U'(\theta) = \xi(t)$.[23] In order to determine the energy landscape $U(\theta)$, we obtained the long-time averaged "equilibrium"occupancy of the rotor as a function of the torsional angle for the different rotor conformations by simulating 11.4 ms trajectories with restrained dihedral angles to prevent the switching between different conformations. The energy landscapes for rotation are then given by relation $k_BT \ln \rho(\theta) \propto U(\theta)$. The landscapes for the two trans-configurations are 6-fold symmetric, with trans-2 shifted by $\pi/6$ rad relative to the trans-1 configuration (Figure 1B), and the landscape for the two cis- configurations are 3-fold symmetric, with cis-2 shifted by $\pi/3$ degrees relative to cis-1 (Figure 1C).

The interaction between the rotor and the gold surface is influenced by a static electric field E_z perpendicular to the gold surface. The partial charges of the DES rotor are distributed such that the negative partial charge of the sulfur ($\delta q_- = -0.335e$) is compensated by the two adjacent methylene groups (each $\delta q_+ = +0.1675e$), leaving the outer methyl groups uncharged. Figure 1B illustrates that since the sulfur is in the rotational axis bound to the gold, the main contribution of the static electric field influencing the rotation is due to a force on the methylene groups. A negative electric field pulls the ethylene away from the gold surface, reducing the torsional barriers slightly compared to the field free state, while a positive electric field presses the methylene groups closer to the gold surface, thus increasing the torsional barriers. Additionally, the field influences the position of the minima and maxima of the energy for the trans-states, with the phase varying by approximately $\pi/60$ radians from -9 to $+9$ V/nm, Figure 2a and b. The amplitude of the energy profile depends on the field for the cis-states, but the phase does not shift.

The energy landscape for the trans-states is a simple cosine function, $U(\theta,E_z) = A(E_z)\cos[n\theta + \phi(E_z)]$ ($n = 3$ for cis- and $n = 6$ for trans-states), at each value of the field, where the field-dependent amplitude is well fit by the relation $A(E_z) = A(0)(1 + aE_z + ...)$, and we keep only the first correction, with $a = 0.058$ nm/V and with $A(0) = k_BT$. The phase relative to the zero-field case is given by $\phi(E_z) = bE_z$, with $b = \pm 0.146$ (nm/V), where we take the minus sign for trans-1 and the plus sign for trans-2. An oscillating electric field normal to the gold surface leads to a time-dependent potential in which both the amplitude $A(E_z(t))$ and phase $\phi(E_z(t))$ vary in time through the external field $E_z(t) = E_0\cos(\omega t)$. In our study the oscillation

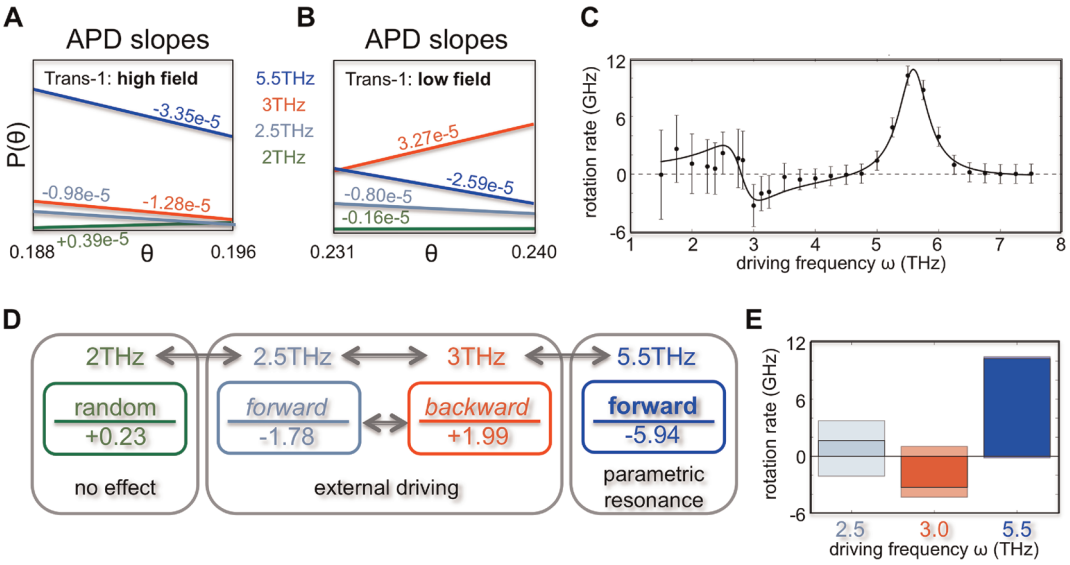

Figure 3. (A,B) Angle probability distributions (APD) of the rotor at different frequency oscillating electric fields (2THz, green; 2.5THz, light blue; 3THz, red; 5.5THz, blue) at the position of the barrier maximum for $E = +9$ V/nm at $\theta = 13.5° \pm 0.25°$ (A) and for $E = -9$ V/nm at $\theta = 11.0° \pm 0.25°$ (B). The colored numbers on the lines are the calculated gradients of the APDs. (C) Each point represents the average response of the rotor in trans-1 conformation over multiple trajectories including the error. The rotor dependence on the driving frequency can be described with eq 2 (solid curve). (D) Scheme correlating the driving frequency to the resulting direction of rotation and the sum of slopes at high and low fields for conformation trans-1. (E) Bar graph illustrating clockwise (positive) and counterclockwise (negative) rotations (pastel colors) and net rotations (vivid colors).

frequency ω ranged from 1.5 to 7.5 THz and the amplitude E_0 ranged from 0.75 to 9 V/nm. These amplitudes, while large, are consistent with the field values in the vicinity of an atomic force microscope (AFM) tip.

Stimulation of the surface rotor by a time-dependent field gives rise to a very rich and complex set of behaviors of the rotor. Neither of the two cis-states undergo directional rotation at any field strength or frequency. The effective rotational diffusion rate, however, does depend significantly on the field parameters. Both trans-1 and trans-2 are driven to undergo directed rotation in a strongly frequency-dependent way. At each frequency the magnitude of the driven rotation is a monotonic function of field amplitude up to about 9 V/nm, so in this paper we focus on the largest field amplitude as we consider the frequency response of the system.

The net rotation rate approaches zero in the zero frequency limit. As the frequency is increased to greater than THz, the rotor begins to undergo net rotation, first one way and then the next, passing through zero. The rotation rate falls back to near zero at slightly higher frequencies. Then, as the frequency increases further, there is a large peak in the net rotational rate. Significantly, the frequency at which the maximum of the high-frequency peak occurs is precisely twice the frequency at which the net rotation goes through zero in switching between clockwise and counterclockwise rotation at the lower frequency feature.

DISCUSSION

We can gain insight into this complex behavior by numerically solving the deterministic equation of motion, which for our sinusoidally oscillating field can be rewritten

$$\ddot{\theta} + \tau^{-1}\dot{\theta} = -\omega_0^2[1 + aE_0\cos(\omega t)][\sin(\theta + bE_0\cos(\omega t))] \quad (1)$$

There are two relevant characteristic frequencies, the damping frequency $\tau^{-1} = \Gamma/I$, and the characteristic librational frequency of the molecule near the minima of the sinusoidal potential $\omega_0 = 2\pi(A(0)/I)^{1/2}/(\pi/3)$. For small molecular rotors the librational frequency is typically on the order of 10^{13} radians/s.[6] Using a moment arm $r = 1$ nm, reduced mass of 15 amu, and an amplitude $A_0 = 4 \times 10^{-21}$ J $\approx k_BT$, we calculate $\omega_0 = 2.4$ THz. Judging by the number of overshoots seen in simulations starting with nonzero initial velocity, the damping frequency τ^{-1} seems to be a bit less than half the librational frequency.

The numerical solution of the deterministic differential eq 1 already foreshadows many of the features observed in the molecular dynamics simulation of the surface rotor. Most notably, for sufficiently large stimulation and for sufficiently small damping, when the external frequency approaches twice the characteristic frequency, there is a period-doubling transition close to $\omega = 2\omega_0$ indicative of parametric resonance. The amplitude of oscillation in the position builds over several periods of the external field, finally reaching a maximum amplitude. The period doubling is similar to the half-synchronous rotation described by Horinek and Michl,[24] although here the amplitude of oscillation—not the rotation rate of the rotor—responds at twice the period of the external stimulation. Inertia is essential for the parametrically driven oscillation, and there is neither period doubling nor increase in amplitude of the oscillation if the

damping is too strong. However, in the absence of driving, inertial effects are damped very quickly, within about 4 overshoot periods ($\sim 10^{-12}$ s^{-1}) with the parameter values we used, as shown in the inset of Figure 2D, consistent with what we observed in the MD simulations. The behavior demonstrated by solving the deterministic eq 1 is not in itself sufficient to explain the observed directed rotation: the ac field acting alone does not provide sufficient energy to overcome the barrier. We propose that the rotation is a noise-assisted stochastic pumping process[25] where the asymmetric oscillation in position leads to a greater chance for thermal activation over the barrier in the clockwise direction than in the counterclockwise direction for the trans-1 state. To emphasize the diffusional character of the motion, we calculated the probability density near the top of the barrier in both high (positive, Figure 3A) and low (negative) field. The net currents can be calculated in terms of the simple diffusion at the top of the barrier averaged over a cycle of the field.

Inspired by the Lorentz model for a bound electron in an oscillating field and by the behavior of a parametric oscillator,[26,27] we search for a theoretical description of the observed features of the induced net rotation in the simulations by cobbling together a linear out-of-phase response function at the characteristic frequency and an in-phase response function at twice the characteristic frequency,

$$J = J_{\max}\left\{\frac{\tau^{-1}(\omega - \omega_0)}{1+[2\tau^{-1}(\omega - \omega_0)]^2} + \frac{1}{1+[2\tau^{-1}(\omega - 2\omega_0)]^2}\right\} \quad (2)$$

Rather amazingly this theory describes the frequency dependence of the net rotation quite well, as shown in Figure 3C. The response at the characteristic frequency arises from a direct driving of the phase (the equilibrium position in a harmonic approximation, Figure 2B), while the response at twice the characteristic frequency arises from parametric modulation of the amplitude (the spring constant in a harmonic approximation, Figure 2B). The essential symmetry breaking occurs because in the trans-1 state the amplitude relative to that at zero-field is large when the phase is negative relative to that at zero field and small when the phase is positive relative to that at zero field, and *vice versa* for trans-2. If either a or b is zero in eq 1, the oscillation is perfectly symmetric under all conditions and there can be no directed rotation even though energy is continually fed into the system *via* the external perturbation.

In the linear driving regime the net rotation is the difference between a large rotation rate in one direction and an even larger rate in the other direction (Figure 3E). On the other hand, in the parametric driving regime the rotation is almost deterministic, with only very infrequent reverse rotations. At still higher frequency both directed and diffusional rotation essentially vanish.

CONCLUSION

We have demonstrated by molecular dynamic simulations that THz applied fields can be used to drive directed motion and to control both rotational diffusion and the magnitude and direction of the net rotation of a diethyl sulfide molecule on a gold surface. Near a characteristic frequency (2.8 THz) that can be calculated from molecular parameters the rotor can be switched between clockwise and counterclockwise rotational modes by small changes in the frequency of the applied field. Unlike a recently described rotor whose direction can be reversed by a chemically induced structural change,[28] here the reversal occurs as the frequency of the applied field is changed. The magnitude of the frequency of the net rotation is 3 GHz, and the Peclet number (the magnitude of the difference divided by the sum of the clockwise and counterclockwise rates) is about 0.5. At twice this characteristic frequency (5.6 THz) the rotor is parametrically pumped to undergo directional rotation at a significantly larger rate (10 GHz) and the Peclet number approaches unity since there are essentially no backward rotations. A simple deterministic model (eq 1) captures qualitatively the observed parametric pumping, but the rotation of the molecule requires thermal noise to provide energy for overcoming the barrier once the large asymmetric oscillation is engendered by the applied field. The frequency response is well described by a simple theory for the response function with an out-of-phase component at the characteristic frequency and an in-phase component at twice the characteristic frequency.

The maximal stimulated net rotation at 10 GHz is very much faster than any other directional rotor with which we are familiar. Although the high frequency seems more likely to have significant technological application, it will be impossible to experimentally access directionality by use of previous mechanisms for sensing directional rotation such as the tunneling current to the surface from an AFM tip. However, the rotating partial charge on the inner methyl groups will cause a magnetic field $\vec{B} = \mu_0\delta_{q+}/Tr$, where μ_0 is the magnetic permeability and T is the period of the rotation. For a maximal rotation rate of 10 GHz this works out to be greater than 10 mG, which should be relatively easily measurable. Conversely, the rotation rate should depend on any magnetic fields, allowing this rotor to act as a molecular compass.[29]

The two distinct trans-states, trans-1 and trans-2, rotate in opposite directions at every frequency and amplitude. With an equal mixture of these two forms on a surface there would be no net rotation. Designing some means of switching the relative stability of the two states would provide a very powerful mechanism for switching the net rotational direction. An interesting possibility is to use a magnetic field normal to the gold surface in combination with a THz field to dynamically favor one state over another, depending on the direction of the magnetic field, even under conditions where the two conformers are *a priori* energetically equivalent. The electric field breaks microscopic reversibility,[30] and the magnetic field then breaks "macroscopic reversibility". A detailed study of the

TABLE 2. Partial Charges Used

group	CH_3	CH_2	S	each H
charge [*e*]	0	+0.1675	−0.335	+0.06

conformational dynamics during stimulation would provide important insight into how to proceed in this direction, but such a study will be very computationally intensive.

We have described a molecular dynamics simulation of a very fast surface rotor that can be sensitively driven and controlled by an external THz ac electric field. We anticipate that this work will provide stimulation for experimental as well as for further theoretical work toward the design of controllable rotors that can be used as components in the design of integrated molecular machines.

METHODS

All simulations of the DES rotor on a gold(111) surface are performed with the MD simulation software GROMACS (Vers. 4.0.x).[31] The GolP force field is used.[32] It is optimized for gold-(111) surface simulations and based on the OPLS-AA force field.[33] The diethyl sulfide parameters have been DFT optimized for this GolP force field by the group of Stephano Corni.[21] The system is simulated in a vacuum with periodic boundary conditions.

The gold is five atom layers thick with a surface area of 3.23 × 3.56 nm^2. The DES is positioned on the surface with the sulfur in an fcc position on the gold 0.258 nm away from each of its three neighboring gold atoms.[34] The position of the sulfur is frozen in space to simulate the sulfur gold bond and to form a stable axis for the stationary rotation on the gold. The gold surface and the DES are both neutrally charged. The partial charge distribution of the DES on the gold can be found in Table 2.

Conflict of Interest: The authors declare no competing financial interest.

Acknowledgment. We thank the German Humboldt Foundation for conferral of a Humboldt Prize to R.D.A. and the Elitenetzwerk Bayern for financial support. J.N. and K.E.G. were supported by Grant 03Z2CN11 (ZIK HIKE) of the Unternehmen Regio Initiative of the BMBF.

Supporting Information Available: System preparation, initial structures, external fields. This material is available free of charge *via* the Internet at http://pubs.acs.org.

REFERENCES AND NOTES

1. Stipe, B. C.; Rezaei, M. A.; Ho, W. Inducing and Viewing the Rotational Motion of a Single Molecule. *Science* **1998**, *279*, 1907–1909.
2. Gimzewski, J.; Joachim, C; Schlittler, R.; Langlais, V; Tang, H; Johannsen, I. Rotation of a Single Molecule within a Supramolecular Bearing. *Science* **1998**, *281*, 531–533.
3. Browne, W. R.; Feringa, B. L. Making Molecular Machines Work. *Nat. Nanotechnol.* **2006**, *1*, 25–35.
4. Coskun, A.; Banaszak, M.; Astumian, R. D.; Stoddart, J. F.; Grzybowski, B. A. Great Expectations: Can Artificial Molecular Machines Deliver on Their Promise?. *Chem. Soc. Rev.* **2012**, *41*, 19–30.
5. Kay, E. R.; Leigh, D. A.; Zerbetto, F. Synthetic Molecular Motors and Mechanical Machines. *Angew. Chem., Int. Ed.* **2007**, *46*, 72–191.
6. Kottas, G. S.; Clarke, L. I.; Horinek, D.; Michl, J. Artificial Molecular Rotors. *Chem. Rev.* **2005**, *105*, 1281–376.
7. Michl, J.; Sykes, E. C. H. Molecular Rotors and Motors: Recent Advances and Future Challenges. *ACS Nano* **2009**, *3*, 1042–1048.
8. Delius, M. v; Leigh, D. A. Walking Molecules. *Chem. Soc. Rev.* **2011**, *40*, 3656–3676.
9. Astumian, R. D. Thermodynamics and Kinetics of a Brownian Motor. *Science* **1997**, *276*, 917–922.
10. Astumian, R. D. Design Principles for Brownian Molecular Machines: How to Swim in Molasses and Walk in a Hurricane. *Phys. Chem. Chem. Phys.* **2007**, *9*, 5067–5083.
11. Klok, M.; Boyle, N.; Pryce, M. T.; Meetsma, A.; Browne, W. R.; Feringa, B. L. MHz Unidirectional Rotation of Molecular Rotary Motors. *J. Am. Chem. Soc.* **2008**, *130*, 10484–10485.
12. Lemouchi, C.; Vogelsberg, C. S.; Zorina, L.; Simonov, S.; Batail, P.; Brown, S.; Garcia-Garibay, M. A. Ultra-Fast Rotors for Molecular Machines and Functional Materials *via* Halogen Bonding: Crystals of 1,4-Bis(iodoethynyl)bicyclo-[2.2.2]octane with Distinct Ggigahertz Rotation at Two Sites. *J. Am. Chem. Soc.* **2011**, *133*, 6371–6379.
13. Kelly, T. R.; DeSilva, H.; Silva, R. A. Unidirectional Rotary Motion in a Molecular System. *Nature* **1999**, *401*, 150–152.
14. Koumura, N.; Zijistra, R. W. J.; Van Delden, R. A.; Harada, N.; Feringa, B. L. Light-Driven Monodirectional Molecule Rotor. *Nature* **1999**, *401*, 152–154.
15. Balzani, V.; Credi, A.; Venturi, M. Light Powered Molecular Machines. *Chem. Soc. Rev.* **2009**, *38*, 1542–1550.
16. Tierney, H. L.; Murphy, C. J.; Jewell, A. D.; Baber, A. E.; Iski, E. V.; Khodaverdian, H. Y.; McGuire, A. F.; Klebanov, N.; Sykes, E. C. H. Experimental Demonstration of a Single-Molecule Electric Motor. *Nat. Nanotechnol.* **2011**, *6*, 625–629.
17. Baber, A.; Tierney, H.; Sykes, E. C. H. A Quantitative Single-Molecule Study of Thioether Molecular Rotors. *ACS Nano* **2008**, *11*, 2385–2391.
18. Tierney, H. L.; Baber, A. E.; Sykes, E. C. H.; Akimov, A.; Kolomeisky, A. B. Dynamics of Thioether Molecular Rotors: Effects of Surface Interactions and Chain Flexibility. *J. Chem. Phys. B* **2009**, *113*, 10913–10920.
19. Vacek, J.; Michl, J. Artificial Surface-Mounted Molecular Rotors: Molecular Dynamics Simulations. *Adv. Funct. Mater.* **2007**, *17*, 730–739.
20. Akimov, A.; Kolomeisky, A. Dynamics of Single-Molecule Rotations on Surfaces that Depend on Symmetry, Interactions, and Molecular Sizes. *J. Phys. Chem. C* **2011**, *40*, 289–313.
21. Iori, F.; Di Felice, R.; Molinar, E.; Corni, S. GolP: an Atomistic Force-Field to Describe the Interaction of Proteins with Au(111) Surfaces in Water. *J. Comput. Chem.* **2009**, *30*, 1465–1476.
22. Tierney, H. L.; Calderon, E. C.; Baber, A. E.; Sykes, E. C. H.; Wang, F. Understanding the Rotational Mechanism of a Single Molecule: STM and DFT Investigations of Dimethyl Sulfide Molecular Rotors on Au(111). *J. Phys. Chem. C* **2010**, *114*, 3152–3155.
23. Gimzewski, J.; Joachim, C.; Schlittler, R.; Langlais, V.; Tang, H.; Johannsen, I. Rotation of a Single Molecule within a Supramolecular Bearing. *Science* **1998**, *281*, 531–533.
24. Horinek, D.; Michl, J. Surface-Mounted Altitudinal Molecular Rotors in Alternating Electric Field: Single-Molecule Parametric Oscillator Molecular Dynamics. *Proc. Natl. Acad. Sci. U. S. A.* **2005**, *102*, 14175–14180.
25. Astumian, R. D. Stochastic Conformational Pumping: A Mechanism for Free-Energy Transduction by Molecules. *Ann. Rev. Biophys.* **2011**, *40*, 289–313.
26. Tan, J.; Gabrielse, G. Parametrically Pumped Electron Oscillators. *Phys. Rev. A* **1993**, *48*, 3105–3122.
27. Alemn, B.; Sussman, A.; Mickelson, W.; Zettl, A. A Carbon Nanotube-Based NEMS Parametric Amplifier for Enhanced Radio Wave Detection and Electronic Signal Amplification. International Symposium "Nanoscience and Quantum Physics 2011". *J. Phys: Conf. Ser.* **2011**, *302*, 012001.
28. Ruangsupapichat, N.; Pollard, M. M.; Harutyunyan, S. R.; Feringa, B. L. Reversing the Direction in a Light-Driven Rotary Molecular Motor. *Nat. Chem.* **2011**, *3*, 53–60.

29. Dominguez, Z.; Khuong, T. A.; Dang, H.; Sanrame, C. N.; Nunez, J. E.; Garcia-Garibay, M. A. Molecular Compasses and Gyroscopes with Polar Rotors: Synthesis and Characterization of Crystalline Forms. *J. Am. Chem. Soc.* **2003**, *125*, 8827–8837.
30. Blackmond, D. G. If Pigs Could Fly Chemistry: A Tutorial on the Principle of Microscopic Reversibility. *Angew. Chem., Int. Ed.* **2009**, *48*, 2648–2654.
31. Hess, B.; Kutzner, C.; van der Spoel, D.; Lindahl, E. GROMACS 4: Algorithms for Highly Efficient, Load-Balanced, and Scalable Molecular Simulation. *J. Chem. Theory Comput.* **2008**, *4*, 435–447.
32. Iori, F.; Corni, S. Including Image Charge Effects in the Molecular Dynamics Simulations of Molecules on Metal Surfaces. *J. Comput. Chem.* **2008**, *29*, 1656–66.
33. Jorgensen, W.; Maxwell, D.; Tirado-Rives, J. Development and Testing of the OPLS All-Atom Force Field on Conformational Energetics and Properties of Organic Liquids. *J. Am. Chem. Soc.* **1996**, *118*, 11225–11236.
34. Tachibana, M.; Yoshizawa, K.; Ogawa, A. Sulfur Gold Orbital Interactions Which Determine the Structure of Alkanethiolate/Au (111) Self-Assembled Monolayer Systems. *J. Phys. Chem. B* **2002**, *106*, 12727–12736.